

# Chapter 16

## Exceptional Discretizations of the NLS: Exact Solutions and Conservation Laws

Sergey V. Dmitriev and Avinash Khare

### 16.1 Introduction

Discrete nonlinear equations that admit exact solutions are interesting from the mathematical point of view and they also help us understand the properties of some physically meaningful discrete nonlinear systems. Completely integrable discrete equations, such as the Ablowitz–Ladik (AL) lattice [1, 2], constitute one class of such equations. Recently, it has been realized by many researchers that *nonintegrable* lattice equations can have subtle symmetries that allow for particular *exact* solutions that propagate with particular velocities and interact with each other inelastically, in contrast to the AL solitons that propagate with arbitrary velocity and collide elastically. For vanishing velocity, one can talk about translationally invariant (TI) stationary solutions (i.e., stationary solutions with arbitrary shift along the lattice). Nonintegrable lattice equations supporting exact moving and/or TI stationary solutions are often called exceptional discrete (ED) models and a natural question is how to identify such models. The problem is often viewed differently, namely, one can look for exceptional solution (not model) parameters when a given lattice equation is satisfied exactly. Exact stationary and moving solutions to nonintegrable discrete nonlinear Schrödinger (DNLS) equations have been constructed and analyzed in a number of recent works [3–14].

In this contribution we first review the existing literature on the exact solutions to the nonintegrable DNLS equations and closely related discrete Klein–Gordon models. Then we report on some analytical and numerical results for the DNLS equations with general cubic nonlinearity.

### 16.2 Review of Existing Works

The search for exact solutions to the nonintegrable DNLS systems has been carried out in two main directions: the first one is the search for DNLS models supporting

---

S.V. Dmitriev (✉)

Institute for Metals Superplasticity Problems RAS, 450001 Ufa, Khalturina 39, Russia  
e-mail: dmitriev.sergey.v@gmail.com

stationary TI solutions, while the second one is the search for exact *moving* solutions to various DNLS equations. Let us summarize the results of those studies.

### 16.2.1 Stationary Translationally Invariant Solutions

The problem at hand can be rephrased as follows: the aim is to discretize the generalized NLS equation of the form

$$i u_t + \frac{1}{2} u_{xx} + G'(|u|^2)u = 0, \quad (16.1)$$

in a way so that the resulting DNLS equation supports the TI stationary solutions. Here  $G(\xi)$  is a real function of its argument and  $G'(\xi) = dG/d\xi$ . It is usually assumed that the DNLS equation that one is looking for has the form

$$i \frac{du_n}{dt} = -\varepsilon \Delta_2 u_n - f(u_{n-1}, u_n, u_{n+1}), \quad (16.2)$$

where  $\Delta_2 u_n \equiv u_{n-1} - 2u_n + u_{n+1}$  is the discrete Laplacian,  $\varepsilon$  is the coupling constant, the nonlinear function  $f$  in the continuum limit ( $\varepsilon \rightarrow \infty$ ) reduces to  $G'(|u|^2)u$  and possesses the property

$$f(ae^{i\omega t}, be^{i\omega t}, ce^{i\omega t}) = f(a, b, c)e^{i\omega t}. \quad (16.3)$$

Seeking stationary solutions of Eq. (16.1) in the form

$$u(x, t) = F(x)e^{i\omega t}, \quad (16.4)$$

we reduce it to an ordinary differential equation (ODE) for the real function  $F(x)$ ,

$$D(x) \equiv \frac{d^2 F}{dx^2} - 2\omega F + 2F G'(F^2) = 0, \quad (16.5)$$

and the problem of finding the ED NLS for (16.1) is effectively reduced to finding the ED forms of the above ODE. Suppose that a discrete analog of Eq. (16.5) that supports TI solutions (with arbitrary shift  $x_0$ ) is found in the form

$$D(F_{n-1}, F_n, F_{n+1}) = 0, \quad (16.6)$$

then the original problem of discretization of Eq. (16.1) can be solved by substituting in Eq. (16.6),  $F_n$  with  $u_n$  or  $u_n^*$  in such a way so as to present it in the form of Eq. (16.2), satisfying the property as given by Eq. (16.3). Usually there are many possibilities to do so.

ED models supporting TI stationary solutions with arbitrary  $x_0$  differ from conventional discrete models supporting only discrete sets of stationary solutions, lo-

cated symmetrically with respect to the lattice, typically in the on-site and inter-site configurations, one of them being stable and corresponding to an energy minimum, while another one being unstable and corresponding to an energy maximum. The energy difference between these two states defines the height of the so-called Peierls–Nabarro potential (PN). TI stationary solutions do not experience this periodic potential and can be shifted quasi-statically along the chain without any energy loss. For the non-Hamiltonian models with path-dependent forces the discussion of the PN energy relief is more complicated but in this case too, zero work is required for quasi-static shift of a TI solution along the path corresponding to continuous change of  $x_0$ .

The problem of discretization of Eq. (16.5) in the form of Eq. (16.6) has been addressed in different contexts, and will be discussed in the rest of this section.

### 16.2.1.1 Integrable Maps

From the theory of integrable maps [15–17] it is known that some of the second-order difference equations of the form of Eq. (16.6) can be integrated, resulting in the first-order difference equation of the form  $U(F_{n-1}, F_n, K) = 0$ , where  $K$  is the integration constant. Such second-order difference equations can be regarded as exactly solvable because the solution  $F_n$  can now be found iteratively, starting from any admissible initial value  $F_0$  and solving at each step the algebraic problem. Continuous variation of the initial value  $F_0$  results in continuous shift  $x_0$  of the corresponding stationary solution along the lattice.

Several years ago, an integrable map was shown to be directly related to the second-order difference equations supporting the Jacobi elliptic function (JEF) solutions [15]. In [16], for the nonlinear equation  $d^2F/dx^2 + aF + bF^3 = 0$ , the discrete analog of the form  $F_{n-1} - 2F_n + F_{n+1} + a[c_{11}F_n + c_{12}(F_{n-1} + F_{n+1})] + b[c_{21}F_{n-1}F_nF_{n+1} + c_{22}F_n^2(F_{n-1} + F_{n+1})] = 0$  was studied and its two-point reduction was found to be of the QRT form [15]. This type of nonlinearity was later studied in [18] and its two-point reduction was rediscovered in [19]. The QRT map appears in many other studies of discrete models, for example, in [11, 20, 21]. Recent results on the integrable maps of the non-QRT type can be found in [17].

One interesting implementation of the theory of integrable maps can be found in [13] where the methodology of [22] was employed. In this work stationary solutions to the DNLS equation with saturable nonlinearity have been analyzed through the corresponding three-point map. It was found that for some selected values of model parameters, the map generates on the plane  $(F_n, F_{n+1})$  a set of points belonging to a line, having topological dimension equal to one. This effective reduction of dimensionality of the map means the possibility of its two-point reduction, resulting in vanishing PN potential.

### 16.2.1.2 Exceptional Discrete Klein–Gordon Equations

Equation (16.5) can be viewed as the static version of the Klein–Gordon equation,  $F_{tt} = F_{xx} - V'(F)$ , with the potential function

$$V(F) = \omega F^2 - G(F^2) . \tag{16.7}$$

Thus, the ED Klein–Gordon equation can be used to write down the ED NLS models (and vice versa).

The first successful attempt in deriving the ED Klein–Gordon equation was made by Speight and Ward [23–25] using the Bogomol’nyi argument [26], and also by Kevrekidis [27]. In both cases, the authors obtained the two-point reduction of the corresponding three-point discrete models. While the Speight and Ward discretization conserves the Hamiltonian, the Kevrekidis discretization conserves the classically defined momentum. These works have inspired many other investigations in this direction [18, 19, 21, 28–36]. Later it was found that both the models can be derived using the discretized first integral (DFI) approach [21, 29].

To illustrate the DFI approach, we write down the first integral of Eq. (16.5),

$$U(x) \equiv (F')^2 - 2\omega F^2 + 2G(F^2) + K = 0 , \tag{16.8}$$

where  $K$  is the integration constant, and discretize it as

$$U(F_{n-1}, F_n, K) \equiv \frac{(F_n - F_{n-1})^2}{h^2} - 2\omega F_{n-1}F_n + 2G(F_{n-1}, F_n) + K = 0 . \tag{16.9}$$

It is assumed that, in the above equation,  $G(F_{n-1}, F_n)$  reduces to  $G(F^2)$  in the continuum limit. On discretizing the left-hand side of the identity  $(1/2)dU/dF = D(x)$ , we obtain the discrete version of Eq. (16.5),

$$D(F_{n-1}, F_n, F_{n+1}) \equiv \frac{U(F_n, F_{n+1}) - U(F_{n-1}, F_n)}{F_{n+1} - F_{n-1}} = 0 . \tag{16.10}$$

Clearly, solutions to the three-point problem  $D(F_{n-1}, F_n, F_{n+1}) = 0$  can be found from the two-point problem  $U(F_{n-1}, F_n, K) = 0$ . We note that Eq. (16.10) was first proposed in [27] and it was used in [3, 10] to derive ED for Eq. (16.1) conserving norm or modified norm and momentum.

### 16.2.1.3 Jacobi Elliptic Function Solutions

Some DNLS equations (and discrete Klein–Gordon equations) with cubic nonlinearity support exact TI stationary [6, 7, 9, 28, 37, 38] and even moving [6, 7, 11] solutions in terms of Jacobi elliptic functions (JEF). Special cases of these solutions describe the TI stationary or moving bright and dark solitons having sech and tanh profiles, respectively. Such solutions can be derived with the help of the JEF identities reported in [39].

JEF solutions are important in their own right, and besides, they also help in establishing the integrable nonlinearities of the QRT type [11]. It is worth pointing out that, so far, no JEF solutions are known to the Kevrekidis ED model given by

Eq. (16.10), thereby indicating that the integrable map to this model is perhaps of the non-QRT type.

An inverse approach to the general problem of finding the kink or the pulse-shaped traveling solutions to the lattice equations was developed by Flach and coworkers [40]. They showed that for a given wave profile, it is possible to generate the corresponding equations of motion. In this context, also see the earlier works [41, 42]. A similar idea has also been used in other studies, see e.g., [43].

## 16.2.2 Exact Moving Solutions to DNLS

Exact moving solutions to the different variants of the DNLS, as was already mentioned, have been derived in terms of the JEF [6, 7, 11]. They have also been found, for DNLS with generalized cubic and saturable nonlinearities, with the help of specially tuned numerical approaches [4, 5, 8, 14]. These works suggest that the moving soliton solutions can be expected in models where, for different model parameters (or/and soliton parameters), there is a transition between stable on-site and inter-site configurations for stationary solitons. Contrary to the DNLS with saturable nonlinearity, the solitons in the classical DNLS do not show such transition and moving solutions have not been found for this system [14].

In our recent work [11] on DNLS with general cubic nonlinearity, we have derived not only moving JEF but also moving sine solutions (also given here in Sect. 16.3). Exact, extended, sinusoidal solutions of the lattice equations have been recently found by several authors [43–47]. It has been proposed that such solutions can be used to construct approximate large-amplitude *localized* solutions by truncating the sine solutions [44, 48].

## 16.3 Cubic Nonlinearity

Here we discuss Eq. (16.2) with the function  $f$  given by

$$\begin{aligned}
 f = & \alpha_1 |u_n|^2 u_n + \alpha_2 |u_n|^2 (u_{n+1} + u_{n-1}) + \alpha_3 u_n^2 (u_{n+1}^* + u_{n-1}^*) \\
 & + \alpha_4 u_n (|u_{n+1}|^2 + |u_{n-1}|^2) + \alpha_5 u_n (u_{n+1}^* u_{n-1} + u_{n-1}^* u_{n+1}) \\
 & + \alpha_6 u_n^* (u_{n+1}^2 + u_{n-1}^2) + \alpha_7 u_n^* u_{n+1} u_{n-1} + \alpha_8 (|u_{n+1}|^2 u_{n+1} + |u_{n-1}|^2 u_{n-1}) \\
 & + \alpha_9 (u_{n-1}^* u_{n+1}^2 + u_{n+1}^* u_{n-1}^2) + \alpha_{10} (|u_{n+1}|^2 u_{n-1} + |u_{n-1}|^2 u_{n+1}) \\
 & + \alpha_{11} (|u_{n-1} u_n| + |u_n u_{n+1}|) u_n + \alpha_{12} (u_{n+1} |u_{n+1} u_n| + u_{n-1} |u_n u_{n-1}|) \\
 & + \alpha_{13} (u_{n+1} |u_{n-1} u_n| + u_{n-1} |u_n u_{n+1}|) \\
 & + \alpha_{14} (u_{n+1} |u_{n-1} u_{n+1}| + u_{n-1} |u_{n-1} u_{n+1}|) ,
 \end{aligned} \tag{16.11}$$

where the real-valued parameters  $\alpha_i$  satisfy the continuity constraint

$$\alpha_1 + \alpha_7 + 2(\alpha_2 + \alpha_3 + \alpha_4 + \alpha_5 + \alpha_6 + \alpha_8 + \alpha_9 + \alpha_{10} + \alpha_{11} + \alpha_{12} + \alpha_{13} + \alpha_{14}) = \pm 2, \quad (16.12)$$

with the upper (lower) sign corresponding to a focusing (defocusing) nonlinearity. Note that Eq. (16.11) is the most general function with cubic nonlinearity which is symmetric under  $u_{n-1} \leftrightarrow u_{n+1}$ .

Particular cases of the nonlinearity (16.11) have been studied in a number of works, many of them are listed in the introduction of [8]. Nonlocal cubic terms coupling the nearest neighbor lattice points naturally appear in the DNLS models approximating continuous NLS with periodic coefficients [49].

### 16.3.1 Conservation Laws

It is easily shown that DNLS Eqs. (16.2) and (16.11) with arbitrary  $\alpha_1, \alpha_4, \alpha_5, \alpha_6, \alpha_{11}, \alpha_{12}$ , with  $\alpha_2 = \alpha_3 + \alpha_8$ , and  $\alpha_7 = \alpha_9 = \alpha_{10} = \alpha_{13} = \alpha_{14} = 0$ , conserve the norm

$$N = \sum_n u_n u_n^*. \quad (16.13)$$

On the other hand, for arbitrary  $\alpha_2, \alpha_{14}$ , with  $\alpha_1 + \alpha_6 = \alpha_4, \alpha_5 = \alpha_6, \alpha_4 + \alpha_5 = \alpha_7, \alpha_8 + \alpha_9 = \alpha_{10}, \alpha_{12} = \alpha_{13}$  and  $\alpha_3 = \alpha_{11} = 0$ , the model conserves the modified norm

$$N_1 = \sum_n (u_n u_{n+1}^* + u_n^* u_{n+1}). \quad (16.14)$$

Instead, if only  $\alpha_7$  is nonzero while all other  $\alpha_i = 0$ , then yet another type of modified norm, given by

$$N_2 = \sum_n (u_n u_{n+2}^* + u_n^* u_{n+2}), \quad (16.15)$$

is conserved.

Further, for arbitrary  $\alpha_2$  and  $\alpha_3$ , with  $\alpha_4 + \alpha_6 = \alpha_1, \alpha_5 = \alpha_6, \alpha_5 + \alpha_7 = \alpha_4, \alpha_9 + \alpha_{10} = \alpha_8$ , and  $\alpha_{11} = \alpha_{12} = \alpha_{13} = \alpha_{14} = 0$ , Eqs. (16.2) and (16.11) conserve the momentum operator

$$P_1 = i \sum_n (u_{n+1} u_n^* - u_{n+1}^* u_n). \quad (16.16)$$

Instead, for arbitrary  $\alpha_5$  and  $\alpha_7$  while all other  $\alpha_i = 0$ , another type of momentum operator, given by

$$P_2 = i \sum_n (u_{n+2} u_n^* - u_{n+2}^* u_n), \quad (16.17)$$

is conserved.

On the other hand, for arbitrary  $\alpha_1, \alpha_4$ , and  $\alpha_6$ , with  $2\alpha_3 = 2\alpha_8 = \alpha_2$ , and  $\alpha_5 = \alpha_7 = \alpha_9 = \alpha_{10} = \alpha_{11} = \alpha_{12} = \alpha_{13} = \alpha_{14} = 0$ , Eq. (16.2) with  $f$  given by Eq. (16.11) can be obtained from the Hamiltonian

$$H = \sum_n \left[ |u_n - u_{n+1}|^2 - \frac{\alpha_1}{2} |u_n|^4 - \frac{\alpha_6}{2} \left[ (u_n^*)^2 u_{n+1}^2 + (u_{n+1}^*)^2 u_n^2 \right] - \alpha_4 |u_n|^2 |u_{n+1}|^2 - \frac{\alpha_2}{2} (|u_n|^2 + |u_{n+1}|^2) (u_{n+1}^* u_n + u_n^* u_{n+1}) \right], \quad (16.18)$$

by using the equation of motion

$$i \dot{u}_n = [u_n, H]_{PB}, \quad (16.19)$$

where the Poisson bracket is defined by

$$[U, V]_{PB} = \sum_n \left[ \frac{dU}{du_n} \frac{dV}{du_n^*} - \frac{dU}{du_n^*} \frac{dV}{du_n} \right]. \quad (16.20)$$

Thus in this model, the energy ( $H$ ) is conserved.

Finally, in case one considers a rather unconventional Poisson bracket given by

$$[U, V]_{PB1} = \sum_n \left[ \frac{dU}{du_n} \frac{dV}{du_n^*} - \frac{dU}{du_n^*} \frac{dV}{du_n} \right] \left[ 1 + (\alpha_2 - \alpha_3) |u_n|^2 + \alpha_8 (|u_{n+1}|^2 + |u_{n-1}|^2) + \alpha_7 u_n (u_{n+1}^* + u_{n-1}^*) + \alpha_7 u_n^* (u_{n+1} + u_{n-1}) \right], \quad (16.21)$$

then the DNLS Eq. (16.2) with  $f$  given by Eq. (16.11) can be obtained from the Hamiltonian

$$H_1 = \sum_n \left[ |u_n - u_{n+1}|^2 - \beta |u_n|^2 \right], \quad (16.22)$$

by using the equation of motion

$$i \dot{u}_n = [u_n, H_1]_{PB1}, \quad (16.23)$$

provided

$$\alpha_7 = 2\alpha_5 = 2\alpha_6, \quad \alpha_8 = \alpha_9 = \alpha_{10}, \quad \alpha_3 = (\beta - 2)\alpha_5, \quad \alpha_4 = (\beta - 2)\alpha_8 + \alpha_5, \\ \alpha_1 = (\beta - 2)(\alpha_2 - \alpha_3), \quad \alpha_{11} = \alpha_{12} = \alpha_{13} = \alpha_{14} = 0. \quad (16.24)$$

Thus the energy ( $H_1$ ) is conserved in this model.

A few summarizing remarks are in order here:

1. In case only  $\alpha_2$  is nonzero while all other  $\alpha_i = 0$ , we have the integrable AL lattice with infinite number of conserved quantities. Among them are, e.g.,  $N_1$ ,  $P_1$ , and  $H_1$  with  $\beta = 2$ , but not  $N$ ,  $N_2$ ,  $P_2$ , and  $H$ .
2. In the case of the conventional DNLS model (i.e., only  $\alpha_1 \neq 0$ ),  $N$  and  $H$  are conserved.
3. The model with only  $\alpha_7$  nonzero conserves  $N_2$  and  $P_2$ .
4.  $N$  and  $P_1$  are conserved in case only  $\alpha_2$  and  $\alpha_3$  are nonzero and  $\alpha_2 = \alpha_3$ .
5.  $N_1$  and  $P_1$  are conserved in case  $\alpha_2$  is arbitrary while  $\alpha_1 = \alpha_4 = \alpha_7$ ,  $\alpha_8 = \alpha_{10}$  while other  $\alpha_i = 0$ .
6. The model conserving  $H$  also conserves  $N$ .
7. The model conserving  $H_1$  also conserves  $N_1$  in case  $\beta = 2$  and  $\alpha_8 = \alpha_9 = \alpha_{10} = 0$ .

### 16.3.2 Two-Point Maps for Stationary Solutions

With the ansatz  $u_n(t) = F_n e^{-i\omega t}$ , we obtain the following difference equation from the DNLS Eqs. (16.2) and (16.11)

$$\begin{aligned} & \varepsilon [F_{n-1} - (2 - \omega/\varepsilon)F_n + F_{n+1}] + \alpha_1 F_n^3 + \gamma_1 F_n^2 (F_{n-1} + F_{n+1}) \\ & + \gamma_2 F_n (F_{n-1}^2 + F_{n+1}^2) + \gamma_3 F_{n-1} F_n F_{n+1} \\ & + \alpha_8 (F_{n-1}^3 + F_{n+1}^3) + \gamma_4 F_{n-1} F_{n+1} (F_{n-1} + F_{n+1}) = 0, \end{aligned} \quad (16.25)$$

where, for convenience, we have introduced the following notation:

$$\begin{aligned} \gamma_1 &= \alpha_2 + \alpha_3 + \alpha_{11}, & \gamma_2 &= \alpha_4 + \alpha_6 + \alpha_{12}, \\ \gamma_3 &= 2\alpha_5 + \alpha_7 + 2\alpha_{13}, & \gamma_4 &= \alpha_9 + \alpha_{10} + \alpha_{14}. \end{aligned} \quad (16.26)$$

In the special case of

$$\alpha_8 = \gamma_4, \quad \alpha_1 = \gamma_2 = \gamma_3, \quad 2\alpha_1 + \gamma_1 + 2\alpha_8 = 1, \quad (16.27)$$

the first integral of the second-order difference Eq. (16.25) reduces to the two-point map

$$\begin{aligned} U(F_{n-1}, F_n, K) &\equiv \varepsilon [(F_{n-1}^2 + F_n^2) - (2 - \omega/\varepsilon)F_{n-1}F_n] \\ &+ \alpha_1 (F_{n-1}^2 + F_n^2) F_{n-1}F_n + \gamma_1 F_{n-1}^2 F_n^2 + \alpha_8 (F_{n-1}^4 + F_n^4) + K = 0, \end{aligned} \quad (16.28)$$

where  $K$  is an integration constant. This is so because Eq. (16.25) can be rewritten in the form



$$\frac{U(F_n, F_{n+1}) - U(F_{n-1}, F_n)}{F_{n+1} - F_{n-1}} = 0, \quad (16.29)$$

and clearly, if  $U(F_{n-1}, F_n) = 0$ , then indeed Eq. (16.25) is satisfied.

On the other hand, in case only  $\gamma_1$  and  $\gamma_3$  are nonzero while  $\alpha_1 = \alpha_8 = \gamma_2 = \gamma_4 = 0$ , then the two-point map is given by

$$W(F_{n-1}, F_n, K) \equiv F_{n-1}^2 + F_n^2 - \frac{Y F_{n-1}^2 F_n^2}{(2 - \omega/\varepsilon)} - 2Z F_{n-1} F_n - \frac{KY}{(2 - \omega/\varepsilon)} = 0, \quad (16.30)$$

which is of the QRT form [15, 16]. Here  $K$  is an integration constant while

$$Z = \frac{(2 - \omega/\varepsilon)^2 - K\gamma_3^2}{2(2 - \omega/\varepsilon) + 2K\gamma_1\gamma_3}, \quad Y = 2\gamma_1 Z + \gamma_3. \quad (16.31)$$

This is because, in this case, Eq. (16.25) can be rewritten in the form

$$\begin{aligned} & \frac{(2 - \omega/\varepsilon)}{2Z(F_{n+1} - F_{n-1})} \left\{ W(F_n, F_{n+1}) - W(F_{n-1}, F_n) \right. \\ & \left. + \frac{\gamma_3}{(2 - \omega/\varepsilon)} [F_{n+1}^2 W(F_{n-1}, F_n) - F_{n-1}^2 W(F_n, F_{n+1})] \right\} = 0, \end{aligned} \quad (16.32)$$

and clearly, if  $W(F_{n-1}, F_n, K) = 0$ , then indeed Eq. (16.3.2) is satisfied. As expected, in the special case of  $\gamma_3 = 0$  so that only  $\gamma_1$  is nonzero, Eq. (16.3.2) reduces to Eq. (16.29).

We want to emphasize that the two-point maps, Eqs. (16.28) and (16.30), allow one to find exact solutions to Eq. (16.25) iteratively, starting from any admissible value of  $F_0$  and solving at each step an algebraic problem. Thus, such solutions define the exact TI stationary solutions to the DNLS Eq. (16.2) with the nonlinearity function  $f$  given by Eq. (16.11).

It is worth pointing out here that some of the exact stationary TI and non-TI solutions (specially the short period and the sine solutions) can also follow from factorized two-point and reduced three-point maps. Several examples of such solutions and their relation with short-period or aperiodic stationary solutions and even with the sine solution can be found in [36]. Here we give two illustrative examples of the TI solutions which follow from factorized two-point and reduced three-point maps.

It is easy to check that Eq. (16.25) has the exact period-four solution

$$F_n = (\dots, a, b, -a, -b, \dots), \quad (16.33)$$

provided

$$2\gamma_2 = \alpha_1 + \gamma_3, \quad (a^2 + b^2)\alpha_1 = 2\varepsilon - \omega. \quad (16.34)$$

Parameter  $a$  in this solution can vary continuously resulting in the shift of the solution with respect to the lattice, which means that this is a TI solution. Now we note that in case

$$\alpha_8 = \gamma_4 = \gamma_1 = 0, \quad \alpha_1 = \gamma_2 = \gamma_3, \quad 2\alpha_1 = 1, \quad K = 2(\omega - 2\varepsilon), \quad (16.35)$$

then the map as given by Eq. (16.28) can be factorized as

$$U(F_{n-1}, F_n) = \frac{1}{2}(2\varepsilon + F_{n-1}F_n) \left( \frac{2\omega}{\varepsilon} - 4 + F_{n-1}^2 + F_n^2 \right) = 0. \quad (16.36)$$

Remarkably, the second factor of this two-point map satisfies the period-four solution (16.33) with the conditions (16.34). Note that the TI solution of Eq. (16.33) is equivalent to the sine solution as given by Eq. (16.50) with  $\beta = \pi/2$  and  $v = k = 0$ .

Our next example is for the model following from the Hamiltonian of Eq. (16.18). In this case, Eq. (16.25) assumes the form

$$\begin{aligned} \varepsilon [F_{n-1} - (2 - \omega/\varepsilon)F_n + F_{n+1}] + \alpha_1 F_n^3 + \gamma_1 F_n^2 (F_{n-1} + F_{n+1}) \\ + \gamma_2 F_n (F_{n-1}^2 + F_{n+1}^2) + \frac{\gamma_1}{3} (F_{n-1}^3 + F_{n+1}^3) = 0. \end{aligned} \quad (16.37)$$

Remarkably, in case the following two-point equation holds

$$F_{n-1}^2 + \frac{4\gamma_1}{3\alpha_1} F_{n-1}F_n + F_n^2 = B, \quad (16.38)$$

then the (stationary) difference Eq. (16.37) can be rewritten as

$$(B\gamma_1 + 3\varepsilon)(F_{n+1} + F_{n-1}) + 3(\omega - 2\varepsilon + B\alpha_1)F_n = 0, \quad (16.39)$$

provided

$$\gamma_2 = \frac{\alpha_1}{2} + \frac{4\gamma_1^2}{9\alpha_1}, \quad B = \frac{\omega - 2\varepsilon - \frac{4\gamma_1\varepsilon}{3\alpha_1}}{\frac{4\gamma_1^2}{9\alpha_1} - \alpha_1}. \quad (16.40)$$

One can now show that for the Hamiltonian model (16.18), the TI stationary sine solutions of Eq. (16.50) with  $v = k = 0$  and with  $v = 0, k = \pi$  also follow from the two-point map (16.38) provided

$$\cos(\beta) = -\frac{2\gamma_1}{3\alpha_1}. \quad (16.41)$$

Furthermore, in this case the three-point Eq. (16.39) is also automatically satisfied.

### 16.3.3 Moving Pulse, Kink, and Sine Solutions

The DNLS model given by Eqs. (16.2) and (16.11) supports exact *moving* JEF solutions, e.g., cn, dn, sn, in case

$$\alpha_1 = \alpha_8 = 0. \quad (16.42)$$

In the limit  $m = 1$ , where  $m$  is the JEF modulus, one obtains the hyperbolic, moving pulse and kink solutions. For  $\alpha_{11} = \alpha_{12} = \alpha_{13} = \alpha_{14} = 0$ , JEF solutions were given in [11] and below we give the hyperbolic and sine solutions including these terms.

In particular, the DNLS model given by Eqs. (16.2) and (16.11) supports the moving pulse (bright soliton) solution,

$$u_n = A \exp[-i(\omega t - kn + \delta)] \operatorname{sech}[\beta(n - vt + \delta_1)], \quad (16.43)$$

provided the parameters satisfy

$$\begin{aligned} v\beta &= 2\varepsilon s_1 S, & \omega &= 2\varepsilon(1 - c_1 C), \\ 2\xi_6 C + \xi_5 &= 0, & [S^2 + (\alpha_3 - \alpha_2)A^2]s_1 &= 0, \\ 2\xi_2 C + \xi_4 &= 0, & A^2(\xi_1 C - \xi_2 + \xi_3/2) &= \varepsilon S^2 C c_1. \end{aligned} \quad (16.44)$$

Here  $\delta$  and  $\delta_1$  are arbitrary constants,  $A$ ,  $\omega$ ,  $k$ ,  $\beta$ , and  $v$  denote the amplitude, frequency, wavenumber, inverse width, and velocity of the moving pulse, respectively, and the following compact notation has been used to describe the relations between the parameters of the exact moving solutions:

$$\begin{aligned} S &= \sinh(\beta), & C &= \cosh(\beta), & T &= \tanh(\beta), \\ s_1 &= \sin(k), & s_2 &= \sin(2k), & s_3 &= \sin(3k), \\ c_1 &= \cos(k), & c_2 &= \cos(2k), & c_3 &= \cos(3k). \\ \xi_1 &= (\alpha_2 + \alpha_3)c_1 + \alpha_{11}, & \xi_2 &= \alpha_4 + \alpha_6 c_2 + \alpha_{12} c_1, \\ \xi_3 &= 2\alpha_5 c_2 + \alpha_7 + 2\alpha_{13} c_1, & \xi_4 &= \alpha_9 c_3 + (\alpha_{10} + \alpha_{14})c_1, \\ \xi_5 &= \alpha_9 s_3 - \alpha_{10} s_1 + \alpha_{14} s_1, & \xi_6 &= \alpha_6 s_2 + \alpha_{12} s_1. \end{aligned} \quad (16.45)$$

From the first expression in Eq. (16.44) it follows that the pulse velocity is zero when  $k = 0$  or  $\pi$ . In the former case we have the nonstaggered, stationary pulse solution while in the latter case, we have the staggered, stationary pulse solution. In particular, for  $v = k = 0$ , the pulse solution is given by

$$u_n = A \exp[-i(\omega t + \delta)] \operatorname{sech}[\beta(n + \delta_1)], \quad (16.46)$$

provided  $2\gamma_2 C + \gamma_4 = 0$ ;  $A^2(\gamma_1 C - \gamma_2 + \gamma_3/2) = \varepsilon S^2 C$ ;  $\omega = 2\varepsilon(1 - C)$ .

On the other hand, the exact moving kink solution to Eqs. (16.2) and (16.11) given by

$$u_n = A \exp[-i(\omega t - kn + \delta)] \tanh[\beta(n - vt + \delta_1)], \quad (16.47)$$

exists provided

$$\begin{aligned} v\beta &= 2\varepsilon s_1 T + \frac{4A^2 \xi_6 T^3}{(1+T^2)}, \quad \frac{(\omega - 2\varepsilon)}{A^2} = \frac{2\xi_1}{S^2} - \frac{2\xi_2}{T^2} + \frac{\xi_3}{T^2}, \\ 2\xi_6 + \xi_5(1+T^2) &= 0, \quad \frac{\varepsilon s_1}{A^2} = -\frac{(\alpha_2 - \alpha_3)s_1}{T^2} - \frac{2\xi_6 T^2}{(1+T^2)}, \\ 2\xi_2 + \xi_4(1+T^2) &= 0, \quad \frac{\varepsilon c_1}{A^2} = -\frac{\xi_1}{T^2} + \frac{\xi_2(1+2T^2 - T^4)}{T^2(1+T^2)} - \frac{\xi_3(1+T^2)}{2T^2}. \end{aligned} \quad (16.48)$$

For  $k = 0$  we obtain the nonstaggered, stationary kink solution

$$u_n = A \exp[-i(\omega t + \delta)] \tanh[\beta(n + \delta_1)], \quad (16.49)$$

provided  $2\gamma_2 + \gamma_4(1+T^2) = 0$ ;  $(\omega - 2\varepsilon)/A^2 = 2\gamma_1/S^2 - (2\gamma_2 - \gamma_3)/T^2$ ;  $\varepsilon/A^2 = -\gamma_1/T^2 - \gamma_3(1+T^2)/(2T^2) + \gamma_2(1+2T^2 - T^4)/[T^2(1+T^2)]$ .

Unlike the JEF and the hyperbolic solutions, the moving as well as the stationary trigonometric solutions of Eqs. (16.2) and (16.11) exist even when all  $\alpha_i$  are nonzero. In particular, the moving sine solution given by

$$u_n = A \exp[-i(\omega t - kn + \delta)] \sin[\beta(n - vt + \delta_1)], \quad (16.50)$$

exists provided the following four relations are satisfied:  $v\beta = -2\varepsilon \sin(\beta)s_1 - 2A^2 \sin^3(\beta)(\alpha_8 s_1 - \xi_5)$ ;  $(\alpha_2 - \alpha_3)s_1 + 2\xi_6 \cos(\beta) - \alpha_8 s_1[4 \sin^2(\beta) - 3] + \xi_5 = 0$ ;  $\alpha_1 + 2(\xi_1 + \xi_4) \cos(\beta) + \xi_3 + 2\xi_2 \cos(2\beta) + 2\alpha_8 c_1 \cos(\beta)[1 - 4 \sin^2(\beta)] = 0$ ;  $\omega - 2\varepsilon + 2\varepsilon c_1 \cos(\beta) = A^2 \sin^2(\beta)[-2\xi_2 + \xi_3 - 6\alpha_8 c_1 \cos(\beta) + 2\xi_4 \cos(\beta)]$ .

### 16.3.4 Stationary TI Solutions

Small-amplitude vibrational spectra calculated for stationary solutions to DNLS satisfying Eq. (16.3) always include a pair of zero-frequency eigenmodes reflecting the invariance with respect to the phase shift. Stationary TI solutions possess two additional zero-frequency modes in their linear spectra (the Goldstone translational modes) [3, 9, 11, 29]. Stationary solutions can be set in slow motion with the use of the TI eigenvectors whose amplitudes are proportional to propagation velocity (see, e.g., [9]). The accuracy of such slowly moving solutions increases with the

decrease in the amplitude of the Goldstone translational mode, i.e., it increases with the decrease in propagation velocity.

Mobility of the bright and the dark solitons at small, as well as at finite velocities have been studied numerically, for the models supporting TI solutions, e.g., in [3, 9, 11]. TI coherent structures are not trapped by the lattice [3] and they can be accelerated by even a weak external field [33].

Properties of solitons in the DNLS with the nearest neighbor coupling in the nonlinear term [as in Eq. (16.11)] differ considerably from the classical DNLS with only  $\alpha_1$  nonzero where there is only on-site nonlinear coupling. For example, the TI dark solitons in case only  $\alpha_2$  and  $\alpha_3$  are nonzero do not survive the continuum limit, while in the classical DNLS they do [9]. On the other hand, in the classical DNLS, only highly localized on-site dark solitons are stable while the inter-site ones are unstable at any degree of discreteness [50, 51]. In the DNLS with only  $\alpha_2$  and  $\alpha_3$  nonzero, TI dark solitons can be robust, movable, and they can survive collisions with each other [9].

To illustrate the above-mentioned features of the stationary TI solutions, in Fig. 16.1 we show slowly moving, highly localized (a) bright and (b) colliding dark solitons (kink and antikink) in the nonintegrable lattices with  $\varepsilon = 1/4$  and (a)  $\alpha_2 = \alpha_3 = \alpha_{11} = 1/3$ , with other  $\alpha_i = 0$ ; (b)  $\alpha_2 = \alpha_3 = 1/2$ , with other  $\alpha_i = 0$ . Space-time evolution of  $|u_n(t)|^2$  is shown and in both cases maximal  $|u_n|^2$  is nearly equal to 1. To boost the solitons we used the zero-frequency Goldstone translational eigenmode with a small amplitude, which is proportional to the soliton velocity [9].

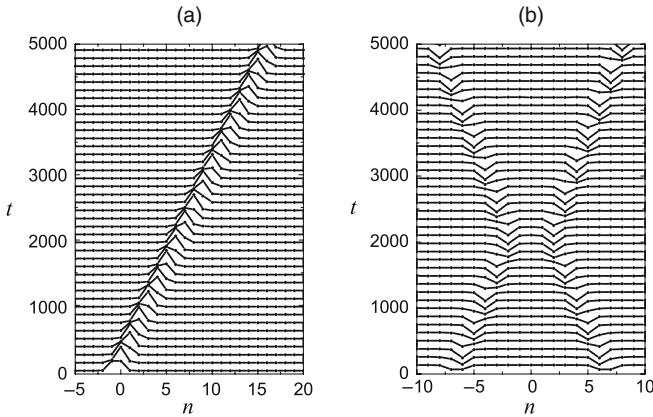


**Fig. 16.1** Space-time evolution of  $|u_n(t)|^2$  showing (a) moving bright and (b) moving and colliding dark solitons (kink and antikink) in nonintegrable lattices. To obtain the slowly moving solitons we used the stationary TI bright and dark soliton solutions supported by the corresponding ED models and boosted them applying the zero-frequency Goldstone translational eigenmode with a small amplitude, which is proportional to the soliton velocity. Parameters are given in the text. (After [9]; © 2007 IOP.)

### 16.3.5 Moving Bright Solitons

Properties of the moving bright solitons with the parameters satisfying (16.44) have been discussed in [11], in case  $\alpha_{11} = \alpha_{12} = \alpha_{13} = \alpha_{14} = 0$ . Here we reproduce some of the results of that work.

From (16.44) it follows that the moving bright soliton solution Eq. (16.43) exists, for example, in case only  $\alpha_3, \alpha_5, \alpha_7$  are nonzero. While the first two relations in (16.44) are always valid [see Fig. 16.2 (a), (b) for the corresponding plots], the other relations and the constraint (16.12) take the form

$$\alpha_3 = \frac{1 - 2\alpha_5 s_1^2}{1 - 2c_1 C}, \quad \alpha_7 = 2(1 - \alpha_3 - \alpha_5), \quad A^2 = \frac{c_1 S^2 C}{1 + \alpha_3(c_1 C - 1) - 2\alpha_5 s_1^2}. \tag{16.51}$$

The number of constraints in this case is such that one has a free model parameter, say  $\alpha_5$ , and pulse parameters  $k$  and  $\beta$  can change continuously within a certain domain [see Fig. 16.2 (c)]. It turns out that in this case, while the nonstaggered stationary pulse ( $k = 0$ ) exists, the staggered stationary pulse ( $k = \pi$ ) does not exist.

On the other hand, in case only  $\alpha_2, \alpha_3, \alpha_5$  are nonzero we have the following constraints:

$$\alpha_3 = -\frac{\alpha_5 c_2}{2c_1 C}, \quad \alpha_2 = 1 - \alpha_3 - \alpha_5, \quad A^2 = \frac{c_1 S^2 C}{(\alpha_2 + \alpha_3)c_1 C + \alpha_5 c_2}. \tag{16.52}$$

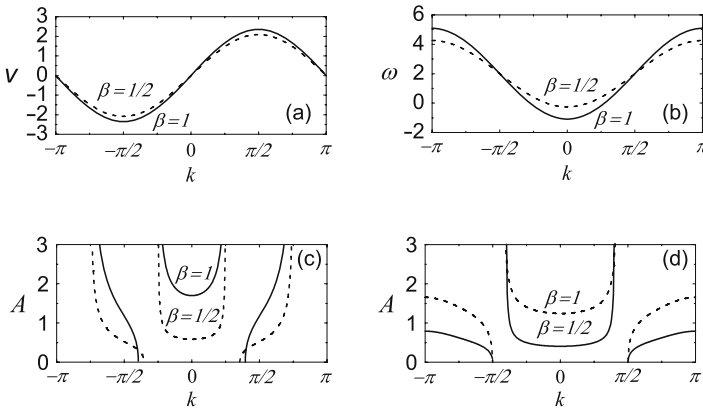


**Fig. 16.2** (a) Velocity  $v$ , (b) frequency  $\omega$ , and (c), (d) amplitude  $A$  of the pulse (bright soliton) as functions of the wavenumber parameter  $k$  at  $\varepsilon = 1$  for the inverse width of the pulse  $\beta = 1/2$  (dashed lines) and  $\beta = 1$  (solid lines). The functions in (a), (b) are defined by the first two expressions in (16.44) and they do not depend on the model parameters  $\alpha_i$ . To plot the amplitude  $A$  we set  $\alpha_5 = 1$  and use (c) (16.51) and (d) (16.52). (After [11]; © 2007 IOP.)

The relation between pulse parameters and model parameters in this case is shown in Fig. 16.2 (d). In this case one has both nonstaggered and staggered stationary pulse solutions in case  $k = 0$  and  $k = \pi$ , respectively.

In both cases, i.e., when Eqs. (16.51) and (16.52) are satisfied, it was found that the stationary bright solitons are generically stable.

The robustness of *moving* pulse solutions, in both these cases, was checked by observing the evolution of their velocity in a long-term numerical run for  $\varepsilon = 1$ . For pulses with amplitudes  $A \sim 1$  and velocities  $v \sim 0.1$  and for various model parameters supporting the pulse,  $|\alpha_i| \sim 1$ , we found that the pulse typically preserves its velocity with a high accuracy. Two examples of such simulations, one for the nonstaggered pulse and another one for the staggered pulse are given in Fig. 16.3 (a), (b) and (a'), (b'), respectively. In (a) and (a') we show the pulse configuration at  $t = 0$  and in (b) and (b') the pulse velocity as a function of time for two different integration steps,  $\tau = 5 \times 10^{-3}$  (solid lines) and  $\tau = 2.5 \times 10^{-3}$  (dashed lines), while a numerical scheme with the accuracy  $O(\tau^4)$  is employed.

In Fig. 16.3 (a,b) and (a',b') we give the numerical results for the pulse solutions given by Eqs. (16.51) and (16.52), respectively. The model characterized by Eq. (16.51) has one free parameter and we set  $\alpha_5 = 1$ . For the pulse parameters we set  $\beta = 1$  and  $k = 0.102102$ . Then we find from the first two expressions in (16.44) and from (16.51) the pulse velocity  $v = 0.239563$ , frequency  $\omega = -1.07009$ , amplitude  $A = 1.7087$ , and the dependent model parameters  $\alpha_3 = -0.473034$  and  $\alpha_7 = 0.946068$ . The model characterized by Eq. (16.52) has one free parameter and

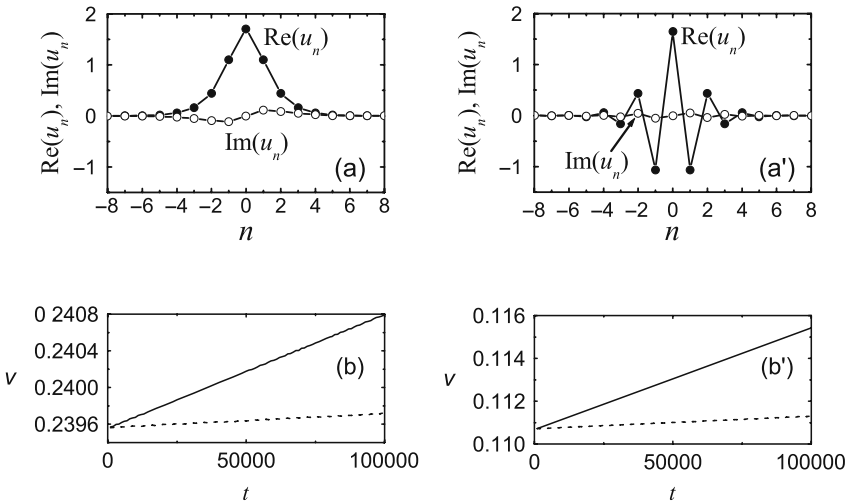


**Fig. 16.3** (a) Nonstaggered moving pulse at  $t = 0$  and (a') same for the staggered pulse. In (b) and (b') the long-term evolution of pulse velocity is shown for the corresponding pulses for the integration steps of  $\tau = 5 \times 10^{-3}$  (solid line) and  $\tau = 2.5 \times 10^{-3}$  (dashed line). Numerical scheme with an accuracy  $O(\tau^4)$  is employed. In both models we find that the pulses preserve their velocity with the accuracy increasing with the increase in the accuracy of numerical integration. Parameters are given in the text. (After [11]; © 2007 IOP.)

we set  $a_5 = 0.3$ . For the pulse parameters we set  $\beta = 1$  and  $k = 3.09447$ . Then we find from the first two expressions in (16.44) and from (16.52) the pulse velocity  $v = 0.110719$ , frequency  $\omega = 5.08274$ , amplitude  $A = 1.65172$ , and the dependent model parameters  $\alpha_2 = 0.603116$  and  $\alpha_3 = 0.0968843$ .

In both cases, one can notice the linear increase in the pulse velocity with time, which is due to the numerical error, since the slope of the line decreases with the decrease in  $\tau$ . The presence of perturbation in the form of rounding errors and integration scheme errors does not result in pulse instability within the numerical run. The velocity increase rate for the staggered pulse in (b') is larger than for the nonstaggered one in (b). This can be easily understood because the frequency of the staggered pulse is almost five times that of the nonstaggered one.

## 16.4 Conclusions and Future Challenges

In this contribution, we have given an overview of the recently reported exact stationary and moving solutions to nonintegrable discrete equations. Such solutions appear to be ubiquitous and they play an important role in our understanding of discrete nonlinear systems.

TI stationary solutions are potentially interesting for applications because they are not trapped by the lattice or, in other words, the PN barrier for them is exactly equal to zero. As a result, they can be accelerated by weak external fields. Such solutions possess the Goldstone translational mode, and thus, they can be boosted along this mode and can propagate at slow speed.

Exact moving solutions to discrete nonlinear equations are interesting in those cases where soliton mobility is an important issue. Such solutions indicate the “windows” in model and/or soliton parameters with enhanced mobility of solitons.

These studies open a number of new problems and research directions. Particularly, it would be interesting to look for the exact TI stationary or moving solutions in discrete systems other than DNLS and discrete Klein–Gordon equation. It would also be of interest to systematically examine the stability and other physical properties of the exact solutions to nonintegrable lattices. Finally, generalizing such approaches to higher dimensions and attempting to obtain analytical solutions in the latter context would constitute another very timely direction for future work.

**Acknowledgments** Our colleagues and friends D. Frantzeskakis, L. Hadžievski, P. G. Kevrekidis, A. Saxena, A. A. Sukhorukov, late S. Takeno, and N. Yoshikawa are greatly thanked for the collaboration on this topic.

## References

1. Ablowitz, M.J., Ladik, J.F.: *J. Math. Phys.* **16**, 598 (1975) 293
2. Ablowitz, M.J., Ladik, J.F.: *J. Math. Phys.* **17**, 1011 (1976) 293
3. Dmitriev, S.V., Kevrekidis, P.G., Sukhorukov, A.A., Yoshikawa, N., Takeno, S.: *Phys. Lett. A* **356**, 324 (2006) 293, 296, 304, 305



4. Melvin, T.R.O., Champneys, A.R., Kevrekidis, P.G., Cuevas, J.: *Physica D* **237**, 551 (2008) 293, 297
5. Melvin, T.R.O., Champneys, A.R., Kevrekidis, P.G., Cuevas, J.: *Phys. Rev. Lett.* **97**, 124101 (2006) 293, 297
6. Khare, A., Rasmussen, K.Ø., Samuelsen, M.R., Saxena, A.: *J. Phys. A* **38**, 807 (2005) 293, 296, 297
7. Khare, A., Rasmussen, K.Ø., Salerno, M., Samuelsen, M.R., Saxena, A.: *Phys. Rev. E* **74**, 016607 (2006) 293, 296, 297
8. Pelinovsky, D.E.: *Nonlinearity* **19**, 2695 (2006) 293, 297, 298
9. Dmitriev, S.V., Kevrekidis, P.G., Yoshikawa, N., Frantzeskakis, D.: *J. Phys. A* **40**, 1727 (2007) 293, 296, 304, 305
10. Kevrekidis, P.G., Dmitriev, S.V., Sukhorukov, A.A.: *Math. Comput. Simulat.* **74**, 343 (2007) 293, 296
11. Khare, A., Dmitriev, S.V., Saxena, A.: *J. Phys. A* **40**, 11301 (2007) 293, 295, 296, 297, 303, 304, 305, 306
12. Maluckov, A., Hadžievski, L., Malomed, B.A.: *Phys. Rev. E* **77**, 036604 (2008) 293
13. Maluckov, A., Hadžievski, L., Stepić, M.: *Physica D* **216**, 95 (2006) 293, 295
14. Oxtoby, O.F., Barashenkov, I.V.: *Phys. Rev. E* **76**, 036603 (2007) 293, 297
15. Quispel, G.R.W., Roberts, J.A.G., Thompson, C.J.: *Physica D* **34**, 183 (1989) 295, 301
16. Hirota, R., Kimura, K., Yahagi, H.: *J. Phys. A* **34**, 10377 (2001) 295, 301
17. Joshi, N., Grammaticos, B., Tamizhmani, T., Ramani, A.: *Lett. Math. Phys.* **78**, 27 (2006) 295
18. Barashenkov, I.V., Oxtoby, O.F., Pelinovsky, D.E.: *Phys. Rev. E* **72**, 35602R (2005) 295, 296
19. Dmitriev, S.V., Kevrekidis, P.G., Khare, A., Saxena, A.: *J. Phys. A* **40**, 6267 (2007) 295, 296
20. Bender, C.M., Tovbis, A.: *J. Math. Phys.* **38**, 3700 (1997) 295
21. Dmitriev, S.V., Kevrekidis, P.G., Yoshikawa, N., Frantzeskakis, D.J.: *Phys. Rev. E* **74**, 046609 (2006) 295, 296
22. Hennig, D., Rasmussen, K.O., Gabriel, H., Bulow, A.: *Phys. Rev. E* **54**, 5788 (1996) 295
23. Speight, J.M., Ward, R.S.: *Nonlinearity* **7**, 475 (1994) 296
24. Speight, J.M.: *Nonlinearity* **10**, 1615 (1997) 296
25. Speight, J.M.: *Nonlinearity* **12**, 1373 (1999) 296
26. Bogomol'nyi, E.B.: *J. Nucl. Phys.* **24**, 449 (1976) 296
27. Kevrekidis, P.G.: *Physica D* **183**, 68 (2003) 296
28. Cooper, F., Khare, A., Mihaila, B., Saxena, A.: *Phys. Rev. E* **72**, 36605 (2005) 296
29. Dmitriev, S.V., Kevrekidis, P.G., Yoshikawa, N.: *J. Phys. A* **38**, 7617 (2005) 296, 304
30. Dmitriev, S.V., Kevrekidis, P.G., Yoshikawa, N.: *J. Phys. A* **39**, 7217 (2006) 296
31. Oxtoby, O.F., Pelinovsky, D.E., Barashenkov, I.V.: *Nonlinearity* **19**, 217 (2006) 296
32. Speight, J.M., Zolotaryuk, Y.: *Nonlinearity* **19**, 1365 (2006) 296
33. Roy, I., Dmitriev, S.V., Kevrekidis, P.G., Saxena, A.: *Phys. Rev. E* **76**, 026601 (2007) 296, 305
34. Dmitriev, S.V., Khare, A., Kevrekidis, P.G., Saxena, A., Hadžievski, L.: *Phys. Rev. E* **77**, 056603 (2008) 296
35. Barashenkov, I.V., van Heerden, T.C.: *Phys. Rev. E* **77**, 036601 (2008) 296
36. Khare, A., Dmitriev, S.V., Saxena, A.: Exact Static Solutions of a Generalized Discrete  $\phi^4$  Model Including Short-Periodic Solutions (2007) arXiv:0710.1460. 296, 301
37. Khare, A., Saxena, A.: *J. Math. Phys.* **47**, 092902 (2006) 296
38. Ross, K.A., Thompson, C.J.: *Physica A* **135**, 551 (1986) 296
39. Khare, A., Lakshminarayan, A., Sukhatme, U.P.: *Pramana (J. Phys.)* **62**, 1201 (2004); math-ph/0306028. 296
40. Flach, S., Zolotaryuk, Y., Kladko, K.: *Phys. Rev. E* **59**, 6105 (1999) 297
41. Schmidt, V.H.: *Phys. Rev. B* **20**, 4397 (1979) 297
42. Jensen, M.H., Bak, P., Popielewicz, A.: *J. Phys. A* **16**, 4369 (1983) 297
43. Comte, J.C., Marquie, P., Remoissenet, M.: *Phys. Rev. B* **60**, 7484 (1999) 297
44. Kosevich, Yu.A.: *Phys. Rev. Lett.* **71**, 2058 (1993) 297
45. Chechin, G.M., Novikova, N.V., Abramenko, A.A.: *Physica D* **166**, 208 (2002) 297
46. Rink, B.: *Physica D* **175**, 31 (2003) 297
47. Shinohara, S.: *J. Phys. Soc. Jpn.* **71**, 1802 (2002) 297
48. Kosevich, Yu.A., Khomeriki, R., Ruffo, S.: *Europhys. Lett.* **66**, 21 (2004) 297

49. Abdullaev, F.Kh., Bludov, Yu.V., Dmitriev, S.V., Kevrekidis, P.G., Konotop, V.V.: Phys. Rev. E **77**, 016604 (2008) 298
50. Fitrakis, E.P., Kevrekidis, P.G., Susanto, H., Frantzeskakis, D.J.: Phys. Rev. E **75**, 066608 (2007) 305
51. Johansson, M., Kivshar, Yu.S.: Phys. Rev. Lett. **82**, 85 (1999) 305